Available online at www.sciencedirect.com

SciVerse ScienceDirect

Ceramics International 38 (2012) 3473–3482

CERAMICS INTERNATIONAL

www.elsevier.com/locate/ceramint

Hydrothermal growth of flower-like CaO for biodiesel production

Fang Liu, Yong Zhang *

School of Materials Science and Engineering, Dalian Jiaotong University, 794 Huanghe Road, 116028 Dalian, PR China

Received 8 August 2011; received in revised form 20 October 2011; accepted 21 December 2011
Available online 31 December 2011

Abstract

Flower-like CaO has been fabricated by a simple hydrothermal approach. Detailed structural characterization revealed that, the flower-like products were constructed by conical-like crystals, with the angle between adjacent lateral edges being 30° or 25°. When flower-like CaO was used as the solid base catalyst to synthesize biodiesel, a high biodiesel yield of 95.5% was achieved. Preferred nucleation and growth of CaO nuclei along [2 2 2] and [4 0 0] growth directions led to conical-like CaO, which coalesced into flower-like architectures by their further contacting and ''welding'' behavior. Flower-like CaO architectures predominantly exposed active O^{2-} on (2 2 2) and (4 0 0) favorable planes of CaO, resulting in obvious enhancement of catalytic activity and high yield of biodiesel.

Keywords: CaO; Hydrothermal; Catalyst; Biodiesel

1. Introduction

Biodiesel, a new kind of alternative energy for transportation sector, is attracting increasing attention because of its renewable, biodegradable and nontoxic advantages [1,2]. Conventionally, biodiesel is produced through the transestrification of triglycerides from vegetable oils and animal fats with monoalkyl alcohols, such as methanol. Due to the noncorrosion, environmental benignancy and easy separation from liquid products advantages, heterogeneous solid base catalysts are being widely used for the transestrification of triglycerides. Among them, CaO is the most widely used and exhibit good catalytic properties for the transesterification of biodiesel [1–4]. However, facile synthesis of effective solid base catalysts to drive the applications of biodiesel is still a big challenge.

Morphology- and structure-controlled growth of micro/nanoarchitectures have attracted much attention, because of their unique physical and chemical properties, leading to promising applications in optical, electrical, magnetic and catalysis fields [5–10]. It is demonstrated that, shape-controlled growth of nanoparticle catalysts, is an important factor to enhance their catalytic properties, because catalytic active planes and active species are predominantly exposed in these cases [8,9]. Our previous result has shown that, controllable growth of ''multi-level tower'' ZnO led to its obvious enhancement of catalytic activity to synthesize biodiesel [10]. Since O^{2-} is the strong basic site in catalytically synthesizing biodiesel [10,11], an interesting idea arises: will shape-controlled growth of unique morphological CaO catalysts be feasible, predominantly exposing catalytic active O^{2-} and effectively improving their catalytic properties? However, the synthesis of calcium oxide is mainly from calcination approach [2,4], with shape-controlled growth of CaO micro/nano structures rarely reported, which limits its marketable applications.

Hydrothermal strategy has exhibited high purity, low cost and easy controlling advantages to synthesize a variety of micro/nano-materials with unique morphologies, such as nanocable [12], nanorod [13], star-shaped and flower-like [14] products, yielding excellent electric, magnetic, optical and catalytic properties. In these cases, organic or inorganic agents are always used to induce the growth of unique morphological micro/nanoarchitectures, which may be helpful for the controllable growth of special morphological CaO and predominant exposure of catalytic active O^{2-} on their favorable planes.

Here, we investigated the hydrothermal growth of flower-like CaO. The growth mechanism of flower-like CaO was proposed, and the influence of CaO morphology upon its catalytic properties to synthesize biodiesel was also discussed.

* Corresponding author. Tel.: +86 0411 84105850.
E-mail address: zhangyong0411@126.com (Y. Zhang).

0272-8842/$36.00
doi:10.1016/j.ceramint.2011.12.061

2. Experimental procedure

In a typical experiment, certain amount of NaOH was dissolved in 70 mL of deionized water. Then, 0.01 mol of $Ca(NO_3)_2{\cdot}9H_2O$ and certain amount of KCl were added to this solution, and treated at 180 °C for 12 h. The obtained solid products were thoroughly washed and filtered by deionized water, then dried at 60 °C.

The morphology of reaction products was observed using energy dispersive spectrometer (EDS) attached scanning electron microscopy (SEM, JSM-6360LV, with an accelerating voltage of 20 kV, secondary electron image), transmission electron microscopy (TEM, H-800, with an accelerating voltage of 200 kV) and high resolution transmission electron microscopy (HRTEM, JEOL2011, with an accelerating voltage of 200 kV). The crystallographic characterization was performed by an X-ray diffraction (XRD, D/Max-Ultima$^+$, with an accelerating voltage of 40 kV,) with Mo Kα radiation at a scanning speed of 6°/min. The FT-IR spectra of the samples were recorded as KBr disks in the wavenumbers region of 500–4000 cm^{-1} with a TENSOR 27 FT-IR spectrometer.

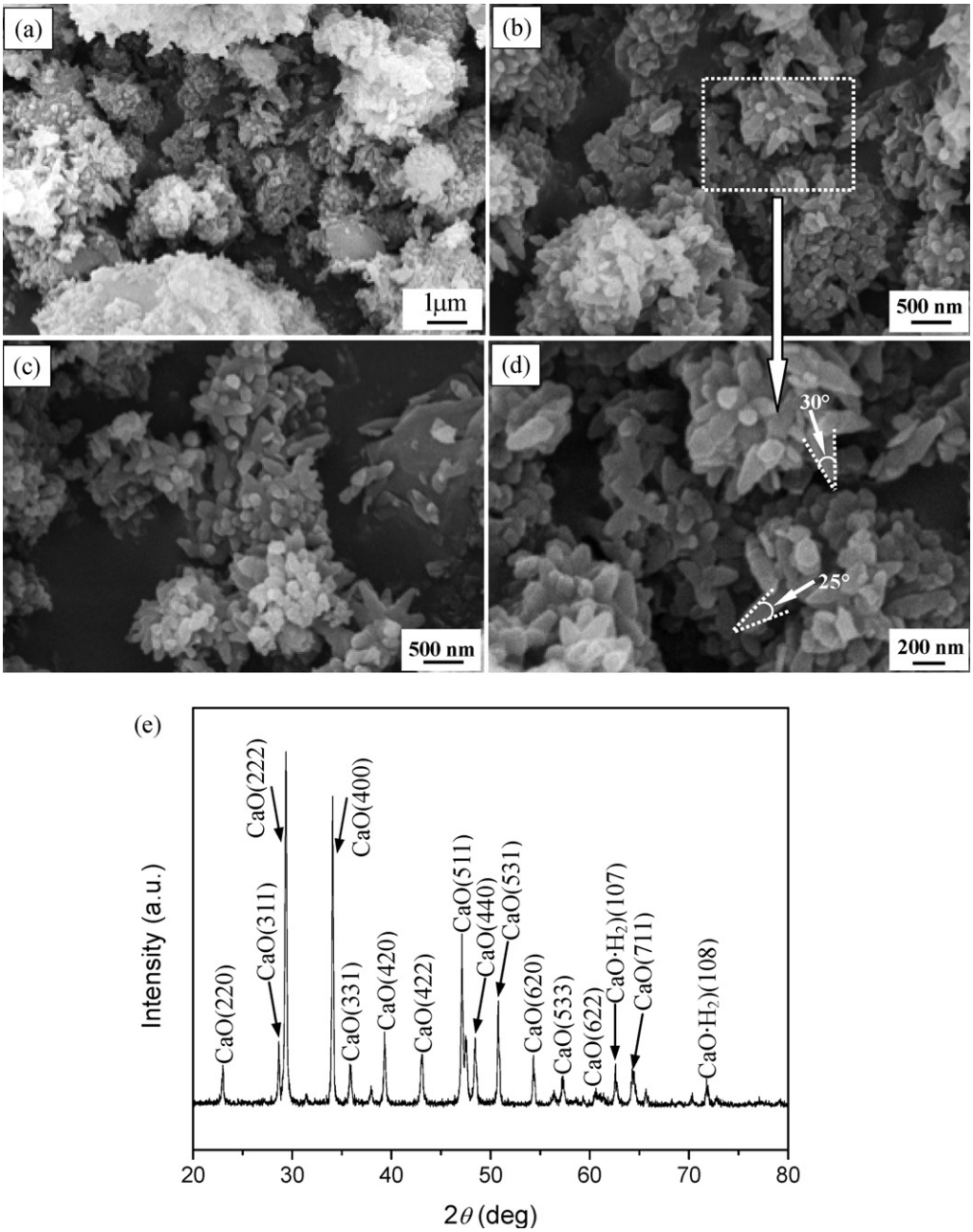

Fig. 1. (a–d) SEM morphology of the as-synthesized product, where, (d) is magnification of the dashed boxed area in (b). (e) XRD pattern of the as-synthesized product.

In reference of previous report [4], the transesterification reactions were carried out in a 100 mL glass reactor with a condenser. Firstly, the solid catalyst was dispersed in methanol under magnetic stirring. Then, soybean oil (AR, Dalian Shenlian Chemical Co., Dalian) was added to the mixture and heated to 60 °C. The magnetic stirring rate was 1000 rpm, and the transesterification lasted for 2 h. Samples were taken out from the reaction mixture every 5 min and solid catalyst was separated by centrifugation. Finally, the excess methanol was distilled off under vacuum. After removal of the glycerol layer, the biodiesel was collected, and the yield of biodiesel was calculated according to the equation of previous report [4].

3. Results and discussion

3.1. Characterization of morphology and structure

SEM observation of the as-synthesized product is shown in Fig. 1(a–d). Abundant aggregated particles are found (Fig. 1(a) and (b)), which exhibit the flower-like morphology, as shown in Fig. 1(c) and (d). The flower-like products are constructed by conical-like crystals, with the angle between adjacent lateral edges being 30° or 25° (Fig. 1(d)). The length and diameter of these conical-like crystals are 0.5–1.0μm and 50–100 nm, respectively.

XRD characterization of the flower-like products (Fig. 1(e)) reveals that, the typical face-centered cubic (FCC) CaO is its main phase (JCPDS card, 01-1160, 17-0912), together with small amount of $CaO{\cdot}H_2O$ found (JCPDS card, 02-0967). As far as CaO is concerned, the strong peaks at 29.43° and 34.21° indicate its preferred growth of (2 2 2) and (4 0 0) planes, respectively (JCPDS card, 01-1160), and the peaks at 28.67° and 39.31° are corresponded to (3 1 1) and (4 2 0) planes of CaO, respectively (JCPDF Card, 01-1160).

In order to understand the growth mechanism of flower-like calcium oxide, its morphology evolution as a function of NaOH amount (0.00 g, 1.00 g and 2.00 g) is examined. When NaOH is not added, no product is achieved in our experiment. When 1.0 g and 2.0 g NaOH are added, the as-synthesized products are shown in Fig. 2. Mostly, irregular-shaped particles of 1–5 μm diameter are obtained, in which small amount of polyhedral particles are found. These results demonstrate that, NaOH is crucial for the mass production of calcium oxide.

Then, different amount of KCl (0.75 g, 1.50 g, 2.25 g) is added into the reaction solution, with the fixed amount of NaOH (1.00 g). For simplicity, these three samples are called sample-0.75, sample-1.50 and sample-2.25 hereafter. As demonstrated in Fig. 3, irregular aggregated products are achieved in sample-0.75, in which ''fluffy'' products are found, as indicated by the white arrows in Fig. 3(a) and (b). When the KCl amount is increased to 1.50 g, flower-like products assembled by conical-like crystals are shown (Fig. 3(c) and (d)). In the case of sample-2.25, abundant flower-like products assembled by conical-like crystals are found, as demonstrated in Fig. 3(e) and (f). These results demonstrate that, the amount of KCl is the key for controlling the morphology evolution of flower-like calcium oxide architectures.

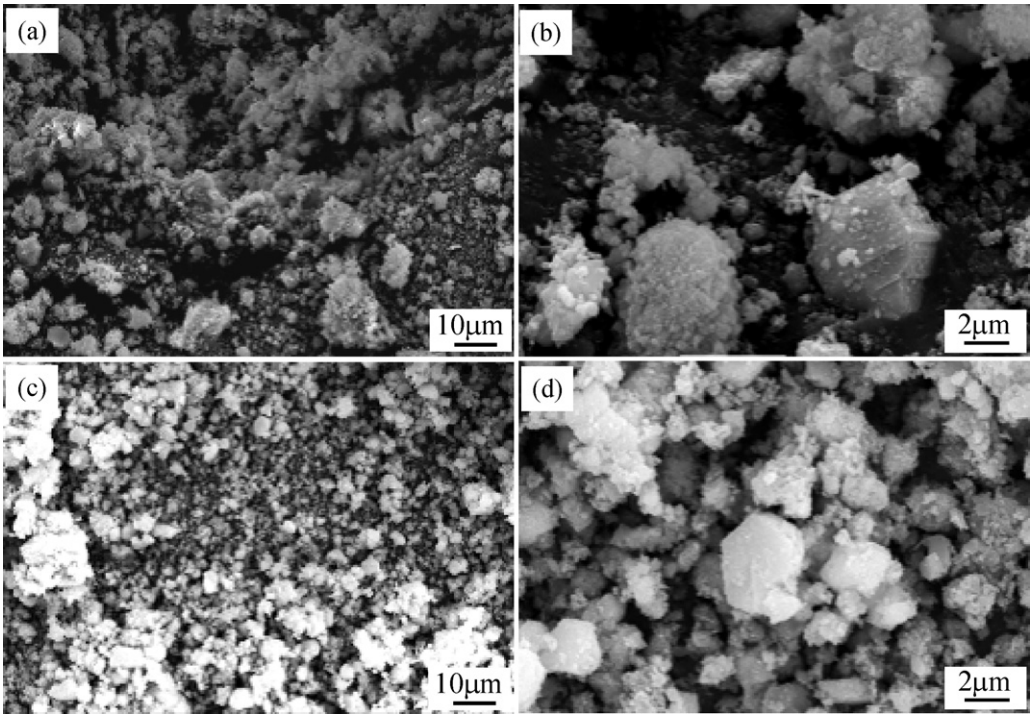

Fig. 2. SEM images of the as-synthesized products at NaOH amount of 1.0 g (a, b) and 2.0 g (c, d).

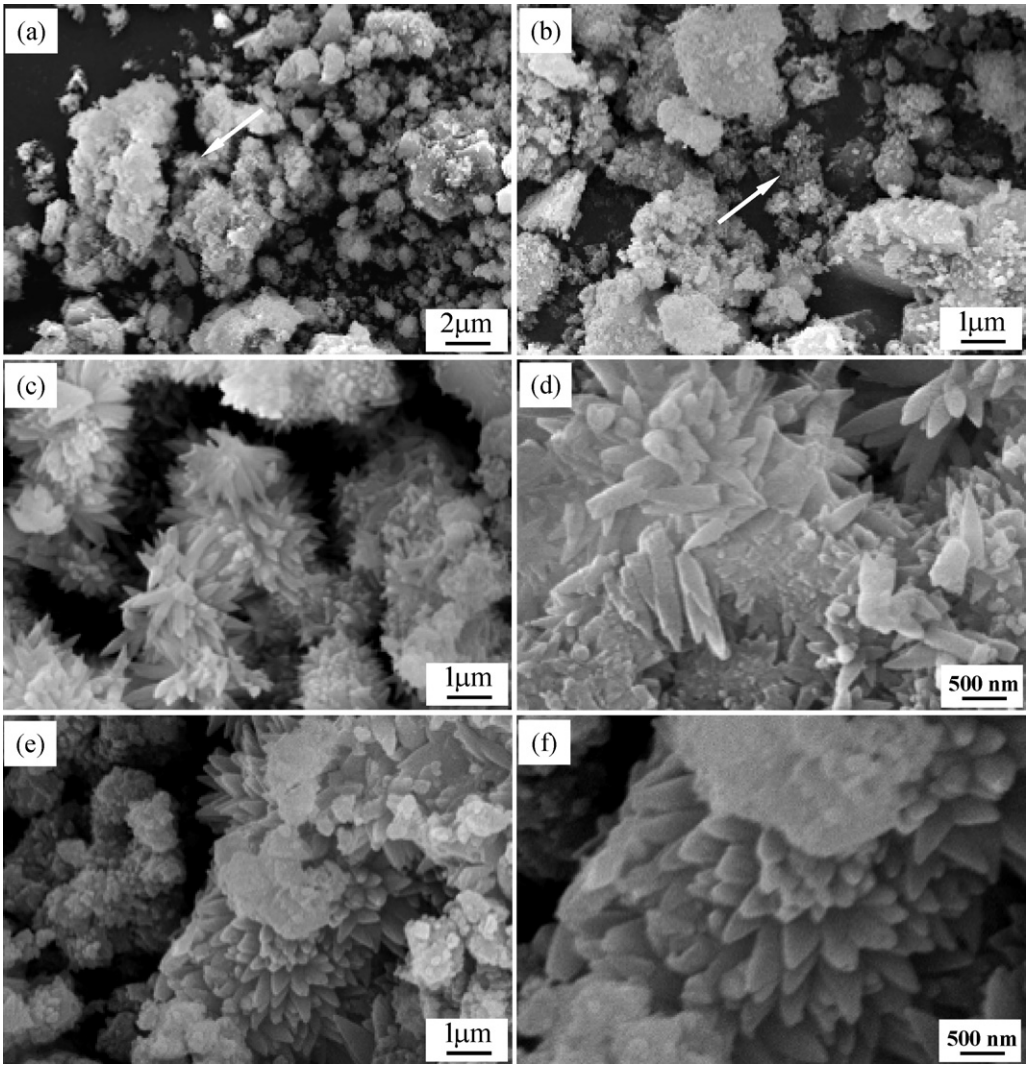

Fig. 3. SEM images of sample-0.75 (a, b), sample-1.50 (c, d) and sample-2.25 (e, f).

Bright field TEM observation of sample-1.50 is shown in Fig. 4(a). The flower-like CaO is connected by conical-like products, in which the conical-like products exhibit wedge-shaped morphology, with the angle between adjacent lateral edges being 25°. Their corresponding electron diffraction pattern (Fig. 4(b)) demonstrates that, $[2\,2\,\bar{2}]$, [2 0 0] and $[1\,3\,\bar{1}]$ are the three growth directions, in agreement with the XRD analysis of Fig. 1(e). Dark field images taken from (2 0 0) and $(2\,2\,\bar{2})$ diffraction spots are shown in Fig. 4(c) and (d), respectively, in which different conical-like products exhibit different brightness, revealing their different crystallographic orientations.

HRTEM observation of sample 1.50 further reflects the facet selective growth character of flower-like CaO. As demonstrated in Fig. 5, conical-like products which exhibit wedge-shaped morphology are found, with the angle between adjacent lateral edges being 30° (Fig. 5(a) and (b)). The interplanar spacings in different areas of conical-like products are about 0.15 nm, 0.12 nm and 0.14 nm (Fig. 5(c–e)), corresponding to the distances between two (3 1 1), (4 0 0) and (2 2 2) planes of CaO, respectively.

3.2. Growth mechanism of flower-like calcium oxide

The facet selective growth of micro/nanoarchitectures is in accordance with the energetically favorable growth principle, which may be helpful to understand the growth mechanism of flower-like CaO. Usually, low index crystal planes of cubic phased nanostructures such as {1 1 1}, {1 0 0} and {1 1 0} planes are more thermodynamically stable than other facets, to fulfill the smallest surface energy principle [15]. Organic or inorganic agents tend to be absorbed by these low index crystal planes, which changes the surface energies of these facets, leading to newly unique morphologies of micro/nanostructures. With the addition of ethylenediamine, ZnO pyramid-like hierarchical micro/nanoarchitectures have been synthesized [16]. When Cl^- is introduced, rod-like ZnO has also been found [17].

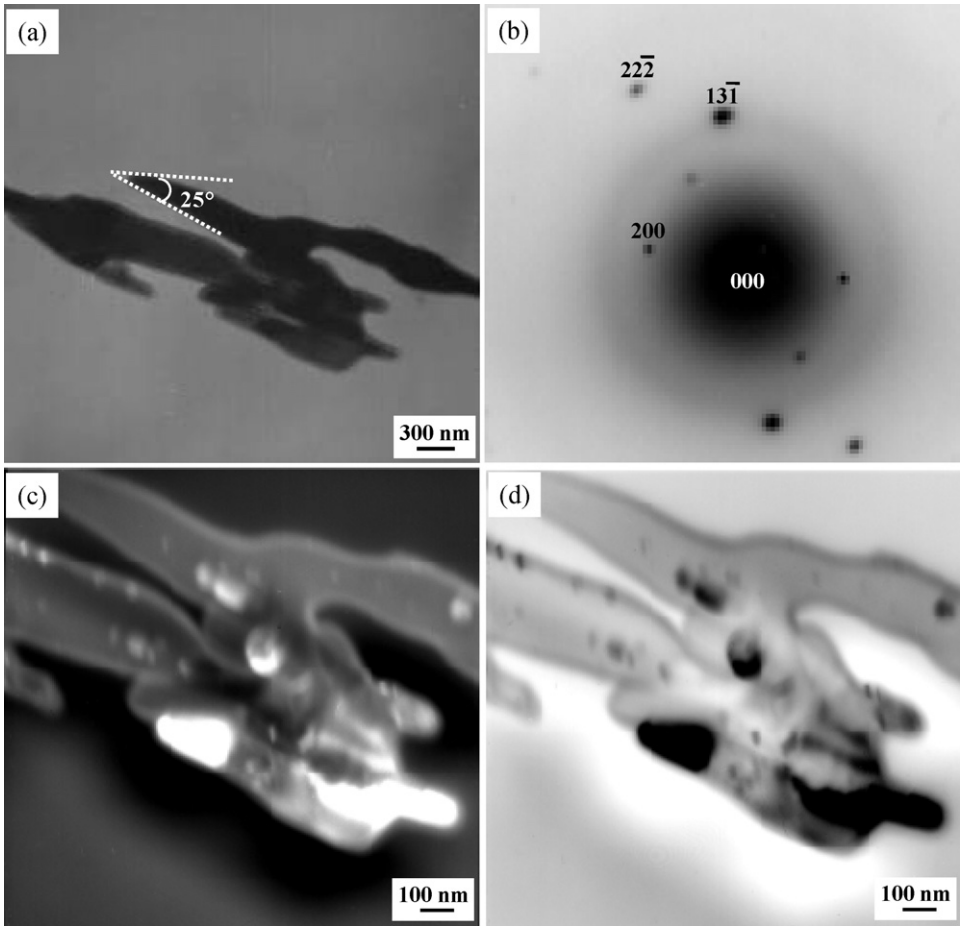

Fig. 4. (a) Bright field TEM images of sample-1.50, with (b) being selected area electron diffraction pattern; (c, d) Dark field TEM images taken from (2 0 0) and $(2\,2\,\bar{2})$ diffraction spots, respectively.

As well known, CaO exhibit a FCC structure. Hence, the most energetically favorable growth planes of {1 1 1}, {1 0 0} and {1 0 1} appear, and the preferred growth of (2 2 2) and (4 0 0) planes of CaO becomes the most energetically favorable. In addition, the secondary energetically favorable growth directions always appear to further reduce the growth surface energy of micro/nanostructures [16–19]. Then, the secondary energetically favorable growth plane of (3 1 1) appears, due to the adsorption of Cl^- on (3 1 1) plane. Consequently, conical-like CaO bounded by (2 2 2) and (3 1 1) planes is achieved, which exhibits the wedge-shaped morphology (Fig. 1), because of the 29° internal angle between (2 2 2) and (3 1 1) planes. Similarly, conical-like CaO bounded by (4 0 0) and (3 1 1) planes is also achieved, because of the 26° internal angle between (4 0 0) and (3 1 1) planes.

Based on the above analysis, the introduction of Cl^- is crucial for the formation of conical-like CaO, thus assembling flower-like product. When 0.75 g KCl is added in the solution, ''fluffy'' products are found after hydrothermal reaction, which indicates the primal microstructure of conical-like CaO. When the KCl amount is 1.50 g and 2.50 g, nucleation and growth of CaO nuclei along [2 2 2] and [4 0 0] directions are completely performed, leading to conical-like nanostructures.

To minimize surface energy, the adjacent conical-like CaO begin to contact each other [7,14]. With the continuous coming of CaO nuclei, the gap area of contacted conical-like structures is filled up. Then, newly arriving CaO nuclei will nucleate and grow up, which ''welds'' the adjacent contacted conical-like structures. Induced by this ''welding'' behavior, more and more conical-like structures coalesce into flower-like architectures, as shown in Fig. 3. The schematic illustration for this growth process is shown in Fig. 6.

According to the experimental results of Yan et al. [18], the diameter of the formed ZnO nanorod is determined by the ratio of its lateral and axial growth rate. Ahsanulhaq et al. [19], also found that, axial [0 0 0 1] and lateral $[1\,0\,\bar{1}\,1]$ directions resulted in nanopencil-like ZnO arrays in solution environment. Similarly, axial [2 2 2] and lateral [3 1 1], as well as axial [4 0 0] and lateral [3 1 1] growth directions lead to conical-like CaO in our experiment, which is confirmed by the above XRD characterization of Fig. 1(e), TEM observation of Fig. 4 and HRTEM results of Fig. 5, respectively.

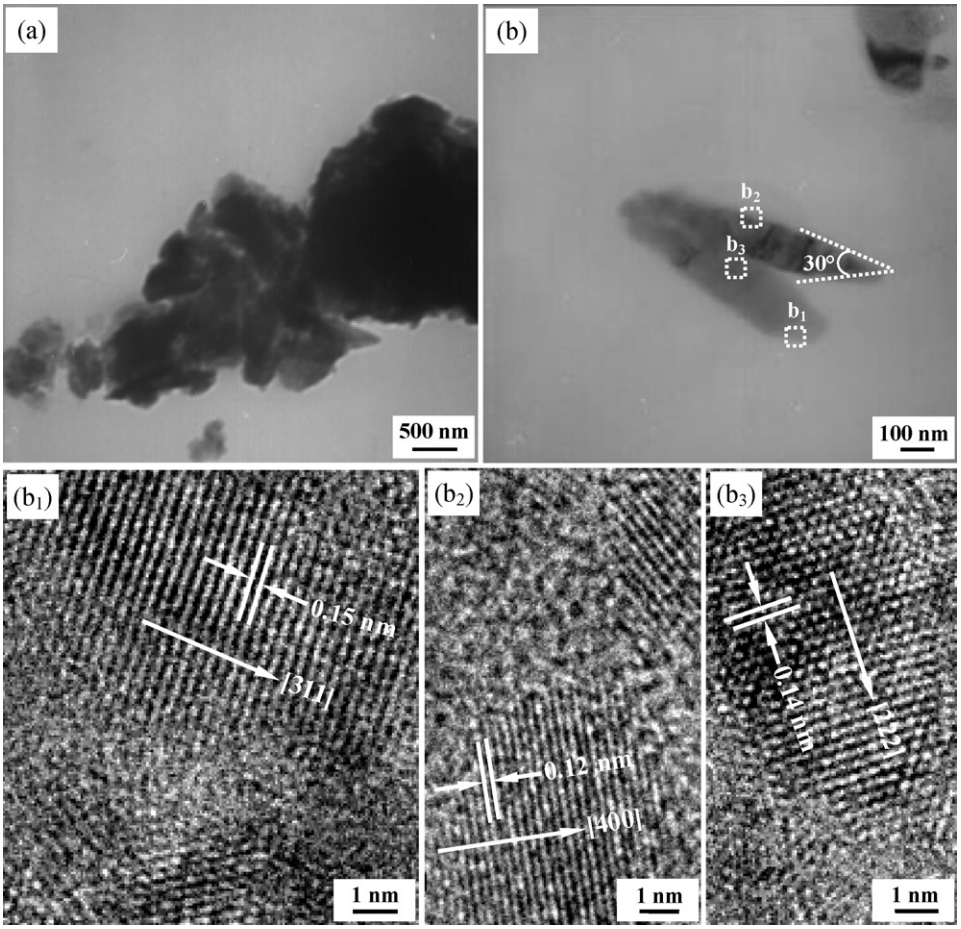

Fig. 5. HRTEM images of sample-1.50, where, (b_1), (b_2) and (b_3) are enlargement of areas b_1, b_2, and b_3 in (b), respectively.

More recently, various flower-like metal oxide, such as ZnO [7], CuO [20], SnO_2 [21], MnO_6 [22] and Y_2O_3 [23] have been reported. Hu et al. [7] reported the hydrothermal growth of star-shaped architectures assembled by conic-like ZnO nanotubes, in which ''welding'' and growth of conic-like ZnO is proposed. 3D flower-like ZnO nanostructures is synthesized by a simple hydrothermal route, and the coalescence of ZnO nanorod to form flower-like architecture is found [14]. The ''welding'' behavior of conical-like structures into flower-like CaO in our experiment is similar with these process, which is confirmed by the continuous interlink of conical-like CaO from different crystallographic orientations (Fig. 4).

In solution environment, the reaction from Ca^{2+} to CaO can be expressed as follows:

$$Ca^{2+} + 2OH^- \rightarrow Ca(OH)_2(s) \rightarrow CaO(s) + H_2O \quad (1)$$

According to reaction (1), $Ca(OH)_2$ is a transitional product in our experiment, which finally transforms to CaO. Then, the amount of NaOH is pivotal for the transformation from calcium hydroxide to calcium oxide. When NaOH is not added, no product is achieved in our experiment. Only after 1.0 g and 2.0 g NaOH are added, the as-synthesized calcium oxides are achieved (Fig. 2).

3.3. Catalytic properties of flower-like CaO in trans-esterification reaction

Different morphologies of CaO are used as solid base catalysts, and the biodiesel yield of different samples is shown in Fig. 7(a). Obviously, sample-1.50 and sample-2.25 exhibit much higher biodiesel yield than that of sample-0.75, and a biodiesel yield of 95.5% is achieved when 2.25 g KCl is added.

Conventionally, biodiesel is produced through the transesterification of triglycerides from vegetable oils and animal fats with mono-alkyl alcohols, such as methanol. Due to the noncorrosion, environmental benignancy and easy separation from liquid products advantages, heterogeneous solid base catalysts such as CaO, SrO and MgO are being widely used for the transestrification of triglycerides [1–4,11,24]. Though numerous solid base catalysts have been reported to produce biodiesel, their marketable applications remain elusive.

Shaped-controlled growth of catalyst nanoparticles is effective to enhance their catalytic activities. Because catalysis reaction is sensitive to certain surface structures of catalyst particles, the catalytic activity can be obviously enhanced on some favorable facets. Hence, it is possible to

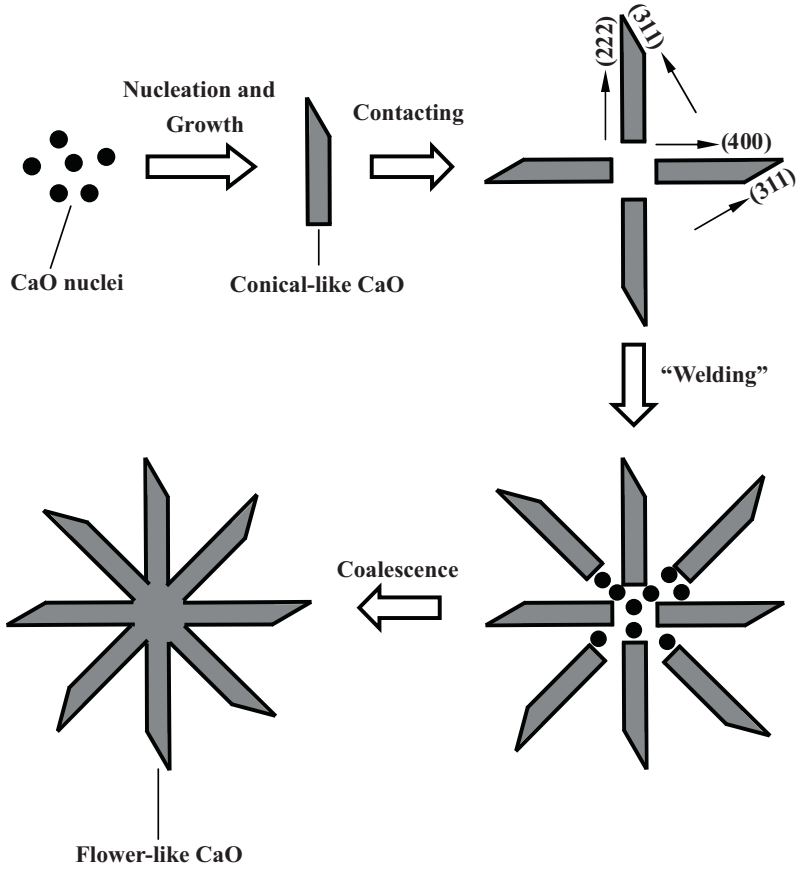

Fig. 6. Schematic illustration for the formation of flower-like CaO.

expose some favorable facets by controlling the shape morphology of catalyst particles [8,9]. It has been shown that, O^{2-} is the predominantly strong basic sites of layer structured Mg–Al hydrotalcites and MgO solid base catalyst to synthesize biodiesel [25]. The lattice oxygens on the surface of ZnO are also considered as basic sites for the transesterification reactions. With the increasing of surface lattice oxygen by La doping, enhanced catalytic properties of ZnO have been reported, with a biodiesel yield of 96.0% achieved [11]. When active O^{2-} is predominantly exposed on (0 0 0 2), $(1\,0\,\bar{1}\,0)$, $(0\,1\,\bar{1}\,0)$ and $(\bar{1}\,1\,0\,0)$ planes of ZnO, its obvious enhancement of catalytic activity to synthesize biodiesel has been achieved [10]. Then, predominant exposure of O^{2-} on favorable facets is promising to enhance the catalytic properties of CaO solid base catalysts.

CaO has a FCC structure, in which the cornual and central points of FCC are occupied by O^{2-} and Ca^{2-}, respectively [26]. Because O^{2-} exhibits larger diameter (0.24 nm) than that of Ca^{2-} (0.20 nm) [27], the framework of FCC structure is regarded as O^{2-} FCC, with the central interstice occupied by Ca^{2-}, as shown in Fig. 7(b). As a result, nine O^{2-} are exposed on {1 1 1} planes, which is the most exposed number of O^{2-}. The exposed number of O^{2-} on {1 0 0}, {0 1 0} and {0 0 1} planes is six, six and five, respectively. According to the structure scheme of Fig. 7(b), the exposure of O^{2-} on (2 2 2), (4 0 0), (3 1 1) and (4 2 0) planes of CaO is compared, which is seven, six, four and three, respectively (Fig. 7(c)). Thus, O^{2-} is predominantly exposed on (2 2 2) and (4 0 0) planes of CaO, favorable to achieve high catalytic activity. When flower-like CaO is used as solid base catalyst to synthesize biodiesel, a high biodiesel yield of 95.5% is achieved (sample-1.50 and sample-2.25). In the case of sample-0.75, no favorable planes exist to predominantly expose active O^{2-}, in which the biodiesel yield is 87.2%.

In order to verify this hypothesis, FT-IR spectroscopy characterization of sample-0.75, sample-1.50 and sample-2.25 is performed, which is shown in Fig. 8. There are strong bands corresponding to hydroxyl groups (O–H) between 2900 and 3500 cm^{-1}. The bands near 2512, 1769, 1435, 875 and 713 cm^{-1} are identified as carboxylate stretches, arising from the adsorption of atmospheric H_2O and CO_2 on the surface of CaO and subsequently formation of $CaCO_3$ [28], respectively, and the bands below 650 cm^{-1} are assigned to the stretching vibrations of Ca–O [29,30]. Obviously, the Ca–O bonds below 650 cm^{-1} in the three samples indicate the existence of flower-like CaO. From 700 cm^{-1} to 2600 cm^{-1}, sample-2.25 and sample-1.50 exhibit much stronger $CaCO_3$ related bands than those of sample-0.75, which reveals the existence of much more flower-like CaO in sample-2.25 and sample-1.50, confirming

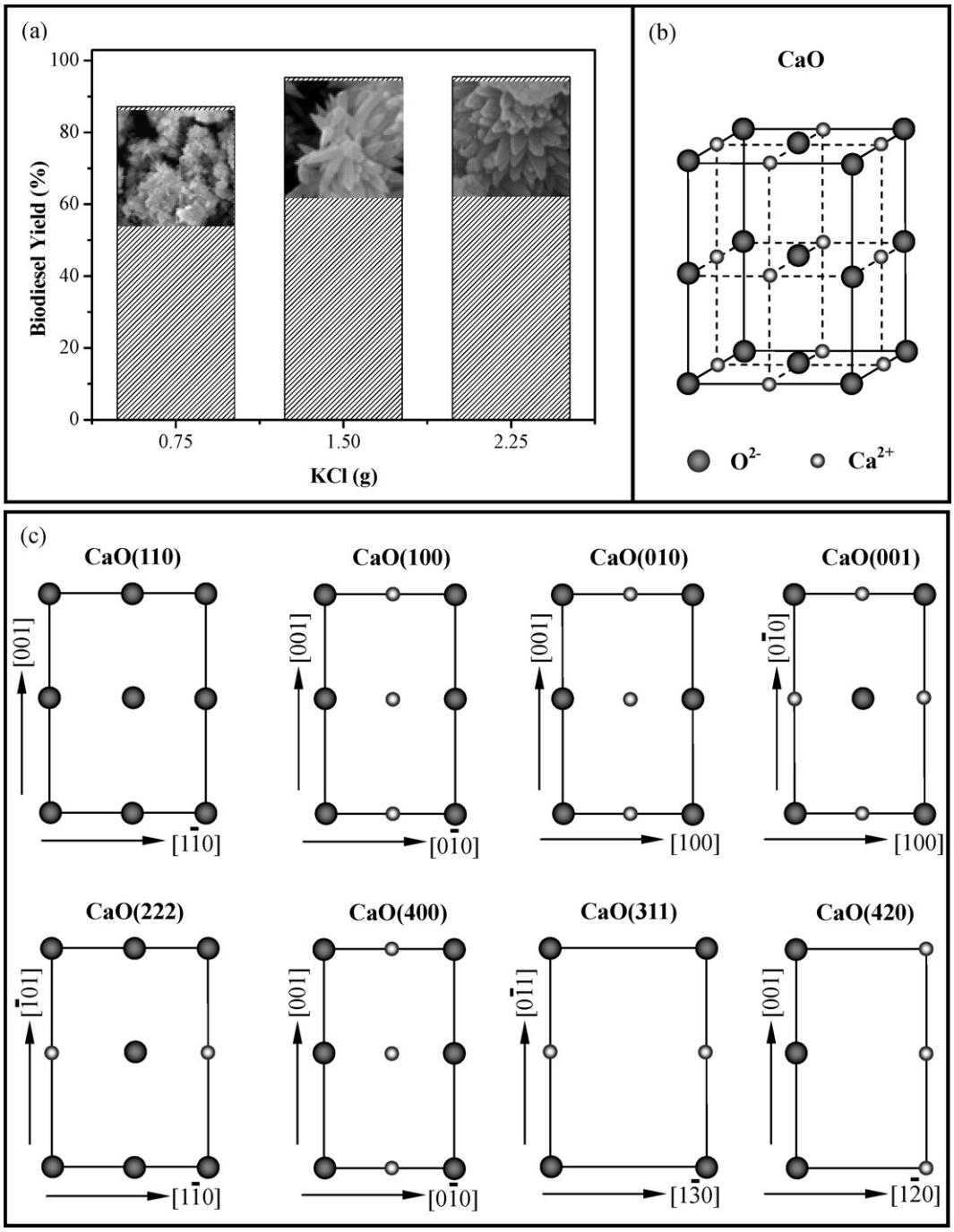

Fig. 7. (a) Biodiesel yield of sample-0.75, sample-1.50 and sample-2.25; (b) Structure model of CaO; (c) surface atomic configurations on the (1 1 0), (1 0 0), (0 1 0), (0 0 1), (2 2 2), (4 0 0), (3 1 1) and (4 2 0) planes of CaO, respectively.

their high catalytic activity in synthesizing biodiesel proposed above.

Recently, the high catalytic activities of CaO to synthesize biodiesel have been widely reported [2,3,29,30], and nanometer scale CaO catalysts for biodiesel production have also been investigated [31]. Our experimental results further reveal that, shape-controlled growth of flower-like CaO to predominantly expose active O^{2-} on (2 2 2) and (4 0 0) favorable planes, leads to obvious enhancement of catalytic activity and high yield of biodiesel. As known, interesting catalytic properties have been achieved from cubic, polyhedral, tripod and other unique morphological micro/nanostructures [8–10]. Structurally induced by organic or inorganic agents, shape-controlled synthesis of unique morphological CaO solid base catalysts to predominantly expose active O^{2-} on favorable planes, may further increase their catalytic activity and accelerate the marketable application of biodiesel.

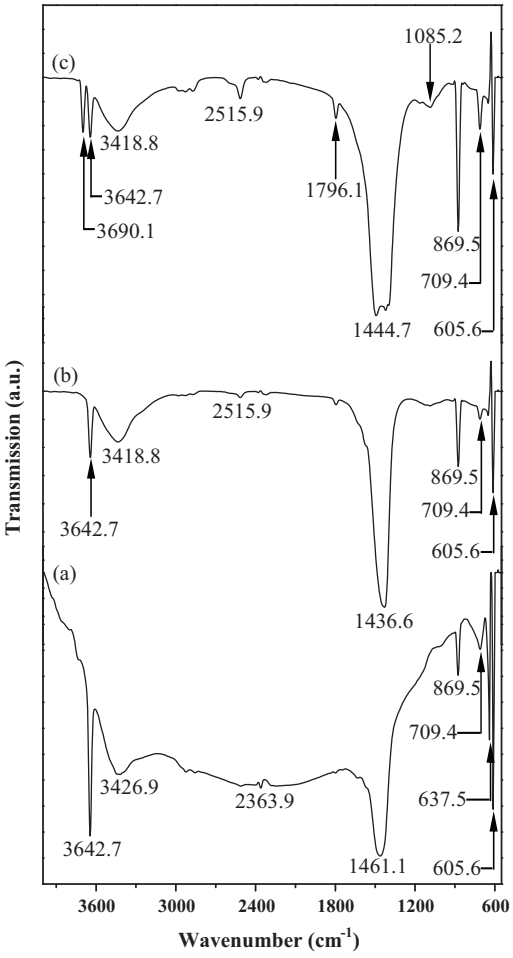

Fig. 8. FT-IR spectra of the sample-0.75 (a), sample-1.50 (b) and sample-2.25 (c).

4. Conclusions

Flower-like CaO with bulk quantity has been fabricated by a simple hydrothermal approach, which were constructed by conical-like crystals, with the angle between adjacent lateral edges being 30° or 25°. Preferred nucleation and growth of CaO nuclei along axial [2 2 2] and lateral [3 1 1], as well as axial [4 0 0] and lateral [3 1 1] growth directions led to conical-like CaO, which coalesced into flower-like architectures by their further contacting and ''welding'' behavior. When flower-like CaO was used as the solid base catalyst to synthesize biodiesel, a high biodiesel yield of 95.5% was achieved, because they predominantly exposed active O^{2-} on (2 2 2) and (4 0 0) favorable planes of CaO, resulting in obvious enhancement of catalytic activity and high yield of biodiesel.

The shape-controlled growth of flower-like CaO architecture in this paper, may give some good suggestions to increase the yield of biodiesel, accelerating its marketable application. Moreover, it may be helpful to fabricate new distinctive morphologies of metal oxide micro/nanostructures, as well as exploring their novel physical and chemical properties.

References

[1] C.S. Cordeiro, C.G.C. Arizaga, L.P. Ramos, F. Wypych, A new zinc hydroxide nitrate heterogeneous catalyst for the esterification of free fatty acids and the transesterification of vegetable oils, Catal. Commun. 9 (2008) 2140–2143.
[2] X.J. Liu, H.Y. He, Y.J. Wang, S.L. Zhu, X.L. Piao, Transesterification of soybean oil to biodiesel using CaO as a solid base catalyst, Fuel 87 (2008) 216–221.
[3] C. Ngamcharussrivichai, P. Totarat, K. Bunyakiat, Ca and Zn mixed oxide as a heterogeneous base catalyst for transesterification of palm kernel oil, Appl. Catal. A 341 (2008) 77–85.
[4] X.J. Liu, H.Y. He, Y.J. Wang, S.L. Zhu, Transesterification of soybean oil to biodiesel using SrO as a solid base catalyst, Catal. Commun. 8 (2007) 1107–1111.
[5] Y.X. Wang, X.Y. Li, G. Lu, G.H. Chen, Y.Y. Chen, Synthesis and photocatalytic degradation property of nanostructured-ZnO with different morphology, Mater. Lett. 62 (2008) 2359–2362.
[6] D.H Fan, R. Zhang, X.H. Wang, Synthesis and ultraviolet emission of aligned ZnO rod-on-rod nanostructures, Solid State Commun. 150 (2010) 824–827.
[7] H.M. Hu, C.H. Deng, X.H. Huang, Hydrothermal growth of center-hollow multigonal star-shaped ZnO architectures assembled by hexagonal conic nanotubes, Mater. Chem. Phys. 121 (2010) 364–369.
[8] X.W. Xie, Y. Li, Z.Q. Liu, M. Haruta, W.J. Shen, Low-temperature oxidation of CO catalysed by Co_3O_4 nanorods, Nature 458 (2009) 746–749.
[9] J.Y. Chen, B. Lim, E.P. Lee, Y.N. Xia, Shape-controlled synthesis of platinum nanocrystals for catalytic and electrocatalytic applications, Nano Today 4 (2009) 81–95.
[10] F. Liu, Y. Zhang, Controllable growth of multi-level tower ZnO for biodiesel production, Ceram. Int. 37 (2011) 3193–3202.
[11] S.L. Yan, S.O. Salley, K.Y. Simon Ng, Simultaneous transesterification and esterification of unrefined or waste oils over ZnO–La_2O_3 catalysts, Appl. Catal. A: Gen. 353 (2009) 203–212.
[12] M.S. Jin, Q. Kuang, Z.Y. Jiang, T. Xu, Z.X. Xie, L.S. Zheng, Direct synthesis of silver/polymer/carbon nanocables via a simple hydrothermal route, J. Solid State Chem. 181 (2008) 2359–2363.
[13] B. Cheng, E.T. Samulski, Hydrothermal synthesis of one-dimensional ZnO nanostructures with different aspect ratios, Chem. Commun. 8 (2004) 986–987.
[14] J.M. Jang, C.R. Kim, H. Ryu, M. Razeghi, W.G. Jung, ZnO 3D flower-like nanostructures synthesized on GaN epitaxial layer by simple route hydrothermal process, J. Alloys Compd. 463 (2008) 503–510.
[15] H.L. Cao, X.F. Qian, C. Wang, X.D. Ma, J. Yin, Z.K. Zhu, High symmetric 18-facet polyhedron nanocrystals of Cu_7S_4 with a hollow nanocage, J. Am. Chem. Soc. 127 (2005) 16024–16025.
[16] F. Lu, W.P. Cai, Y.G. Zhang, ZnO hierarchical micro/nanoarchitectures: solvothermal synthesis and structural enhanced photocatalytic performance, Adv. Funct. Mater. 18 (2008) 1047–1056.
[17] F. Xu, Y.N. Lu, Y. Xie, Y.F. Liu, Controllable morphology evolution of electrodeposited ZnO nano/micro-scale structures in aqueous solution, Mater. Des. 30 (2009) 1704–1711.
[18] Y.G. Yan, L.X. Zhou, Z.D. Han, Y. Zhang, Growth analysis of hierarchical ZnO nanorod array with changed diameter from the aspect of supersaturation ratio, J. Phys. Chem. C 114 (2010) 3932–3936.
[19] Q. Ahsanulhaq, A. Umar, Y.B. Hahn, Growth of aligned ZnO nanorods and nanopencils on ZnO/Si in aqueous solution: growth mechanism and structural and optical properties, Nanotechnology 18 (2007) 115603.
[20] F. Teng, W.Q. Yao, Y.F. Zheng, Y.T. Ma, Y. Teng, T.G. Xu, S.H. Liang, Y.F. Zhu, Synthesis of flower-like CuO nanostructures as a sensitive sensor for catalysis, Sens. Actuators B 134 (2008) 761–768.
[21] Z.R. Li, X.L. Li, X.X. Zhang, Y.T. Qian, Hydrothermal synthesis and characterization of novel flower-like zinc-doped SnO_2 nanocrystals, J. Cryst. Growth 291 (2006) 258–261.
[22] D. Yan, P.X. Yan, G.H. Yue, J.Z. Liu, J.B. Chang, Q. Yang, D.M. Qu, Z.R. Geng, J.T. Chen, G.A. Zhang, R.F. Zhuo, Self-assembled flower-like

hierarchical spheres and nanobelts of manganese oxide by hydrothermal method and morphology control of them, Chem. Phys. Lett. 440 (2007) 134–138.

[23] S.Y. Zeng, K.B. Tang, T.W. Li, Z.H. Liang, 3D flower-like Y_2O_3: Eu^{3+} nanostructures: template-free synthesis and its luminescence properties, J. Colloid Inter. Sci. 316 (2007) 921–929.

[24] J.M. Marchetti, V.U. Miguel, A.F. Errazu, Possible methods for biodiesel production, Renew. Sust. Energy Rev. 11 (2007) 1300–1311.

[25] J.J. Di Cosimo, V.K. Diez, M. Xu, E. Iglesia, C.R. Apesteguia, Structure and surface and catalytic properties of Mg–Al basic oxides, J. Catal. 178 (1998) 499–510.

[26] R.N. Carlos, R.A. Encarnacion, L. Ana, B.R.N. Alejandro, O.H. Miguel, Thermal decomposition of calcite: mechanisms of formation and textural evolution of CaO nanocrystals, Am. Mineral. 94 (2009) 578–593.

[27] R.C. Weast, Handbook of Chemistry and Physics, 84th ed., CRC Press, USA, 2003.

[28] R.A. Nyquist, R.O. Kagel, Infrared Spectra of Inorganic Materials, Academic Press, New York and London, 1971.

[29] C.G.A. Monica, C.S.A. Diana, L.C. Celio, S.G. Jose, M.M.R. Josefa, M.T. Ramon, R.C. Enrique, J.L. Antonio, M.T. Pedro, Transesterification of ethyl butyrate with methanol using MgO/CaO catalysts, J. Mol. Catal. A 300 (2009) 19–24.

[30] C.A.R. Ana, S.G. Jose, M.M.R. Josefa, M.T. Ramon, M.A. David, J.L. Antonio, M.T. Pedro, Heterogeneous transesterification processes by using CaO supported on zinc oxides as basic catalysts, Catal. Today 149 (2010) 281–287.

[31] C. Liu, P.M. Lv, Z.H. Yuan, F. Yan, W. Luo, The nanometer magnetic solid base catalyst for production of biodiesel, Renew. Energy 35 (2010) 1531–1536.